Journal of Atmospheric and Solar-Terrestrial Physics 89 (2012) 120–131

Contents lists available at SciVerse ScienceDirect

Journal of Atmospheric and Solar-Terrestrial Physics

journal homepage: www.elsevier.com/locate/jastp

Implications of the visual appearance of ball lightning for luminosity mechanisms

Karl D. Stephan *

Ingram School of Engineering, Texas State University-San Marcos, San Marcos, TX 78666, USA

ARTICLE INFO

Article history:
Received 24 January 2012
Received in revised form
21 August 2012
Accepted 2 September 2012
Available online 11 September 2012

Keywords:
Ball lightning
Luminosity
Lightning
Radiative transfer theory

ABSTRACT

Observations of ball lightning continue to pose one of the more difficult unsolved problems in atmospheric physics. Lack of quantitative data has frustrated attempts to explain how the objects emit light. We examine three leading theories for the immediate cause of light emission: excitation of plasma, small hot individual particles suspended in air, and hot fractal clusters of small particles. Using radiative transport theory, we find quantitative values for the ranges of particle density and temperature required to produce luminous intensities consistent with the bulk of reported observations, as well as estimates of power requirements for each mechanism. We conclude that all of these mechanisms are consistent with many ball-lightning observations, and that more than one of them may be involved in the luminosity of ball lightning.

1. Introduction

Ball lightning is one of the few remaining unsolved puzzles of atmospheric physics. While scientific studies of ball lightning date back at least to the time of D. F. J. Arago, who published a short study of twenty reports of ball lightning in 1838 (cited in Stenhoff, 1999, p. 3), the scientific literature on ball lightning consists largely of (1) fortuitous reports and observations by mostly untrained personnel, many of which are subject to a variety of interpretations, and (2) theories, many of which explain only one or a few of the fairly consistent set of characteristics that emerge from observations of ball lightning in nature. Relatively little experimental research has been published on the subject of ball lightning, either in the form of field observations with specialized equipment or laboratory experiments designed to reproduce the phenomenon. The consensus of opinion on laboratory experiments so far is that, although some characteristics of ball lightning can be reproduced, no experiment has successfully and repeatably reproduced the phenomenon so that the experimental result is consistent with all four of the following essential characteristics of ball lightning (Rakov and Uman, 2003, p. 662–663):

(i). "ball lightning's association with thunderstorms or with cloud-to-ground lightning;
(ii). its reported shape, diameter, and duration, and the fact that its size, luminosity, and appearance generally do not change much during its lifetime;
(iii). its occurrence in both open air and in enclosed spaces such as building or aircraft;
(iv). the fact that ball lightning motion is inconsistent with the convective behavior of a hot gas;…."

In the thousands of recorded eyewitness reports of ball lightning (hereinafter abbreviated BL), (e.g., Amirov and Bychkov., 1994; Stenhoff, 1999; Barry, 1980; Singer, 1971; and references therein) the following salient characteristics emerge as consistent themes. The BL object typically appears in association with thunderstorms, either immediately after a local lightning strike or while lightning activity is present in the vicinity. Once it is sighted, the lifetime of the BL object can range from less than 1 to 10 s or more, although most eyewitnesses report durations shorter than 1 min (Stenhoff, 1999, p. 14). A BL object generally appears to be a glowing, roughly spherical shape suspended in air, with a median diameter of about 25 cm (Stenhoff, 1999, p. 13–14). As indicated above, BL objects usually do not rise vertically as a heated gas would do, but exhibit a variety of motions, including slow or rapid horizontal movement, stationary hovering, downward motions, and the execution of turns and even reversals of direction (Abrahamson et al., 2002a). When eyewitnesses attempt to estimate brightness, the usual standard of comparison is a frosted incandescent lamp, probably because it is a familiar object whose shape and diffuse light emission most closely resembles the appearance of BL (Charman, 1979). Another quite common observation is that when eyewitnesses address the question of whether the BL object was opaque, translucent, or transparent, opacity is sometimes mentioned. This is a notable characteristic for an object that is apparently no denser than air and fairly small. While it is difficult to quantify this assertion statistically without extensive research in large databases of BL sightings, a sampling

* Corresponding author. Tel.: +1 512 2453060; fax: +1 512 2453052.
E-mail address: kdstephan@txstate.edu

1364-6826/$ - see front matter © 2012 Elsevier Ltd. All rights reserved.
http://dx.doi.org/10.1016/j.jastp.2012.09.001

of several brief reports or compilations of ball-lightning reports (Abrahamson et al., 2002a; Grigor'ev et al., 1992; Jennison, 1969) shows that the question of opacity or transparency is usually not addressed by the observers. Two of fourteen reports mention transparency, one mentions opacity, and the rest do not report whether or not background features were visible through the BL object.

Another important characteristic of interest in eyewitness reports is the apparent brightness of the BL object. As Charman points out (Charman, 1979), the unaided eye is a poor instrument to use for absolute photometry. Perceived brightness of an object can be influenced by many factors: illumination of the surroundings, color contrasts or similarities, motion, duration, and subjective factors such as visual acuity and dark adaptation of the retina. However, the question of whether or not a thing emits light is accurately answered by most observers because shadows, backgrounds illuminated by the object, and other visual cues usually provide enough information to allow the observer to reach the correct conclusion. Another question that observers can answer (although relatively few BL reports explicitly address it) is whether any features of the background can be observed through the BL object. A few reports mention such translucency or transparency, although the vast majority do not, and some explicitly use terms such as "solid," "opaque" and similar words to convey the impression that it was not possible to see through the BL object to the background.

If a self-illuminated object prevents visualization of a scene behind it, at least one of two factors (and possibly both) is at work: (1) the object is absorbing and/or scattering enough light from the background so that any remaining transmitted background light is rendered invisible, or (2) while the object does not itself absorb or scatter significant background light, its own light output is great enough to overwhelm the transmitted background light and reduce it to invisibility. An example of the former case (1) is a dense fog at night, which emits no light of its own but scatters or absorbs light emitted from other objects. An example of the latter case (2) is a candle flame. It is not possible to see objects behind a candle flame in darkness or ordinary interior room lighting, but if a brightly-illuminated background is viewed through a candle, the flame becomes almost invisible and therefore effectively transparent (see Fig. 1).

Through the use of radiative transport theory, these notions can be expressed in quantitative terms and used to set bounds on certain optical characteristics that BL objects must show in order to produce the observed phenomena, including opacity, transparency, or an intermediate condition. We can also use radiative transport theory to arrive at quantitative conclusions about the nature of the light-emission mechanisms in BL objects, as the following discussion will show.

2. Radiative transport theory applied to ball lightning

Radiative transport theory was developed to explain why atomic spectral lines were observed in emission in some stars and absorption in others (Schuster, 1905). It treats radiation by means of an energy-conservation approach, rather than by explicitly solving Maxwell's equations, and therefore is an approximation to an exact solution. However, radiative transport theory has been employed successfully in a wide range of problems ranging from radar backscattering to optical phenomena (Ishimaru, 1978).

The fundamental unit of measure in radiative transport theory is the specific intensity of a ray of electromagnetic energy. (Although polarization can be treated with this theory, we will neglect polarization in the present analysis.) In a vacuum near a radiating surface, the specific intensity due to emission of radiation from a differential surface area da to which the unit vector $\hat{s}_0$ is perpendicular, at a point $\vec{r}$ in a direction $\hat{s}$ from the area is defined as (Ishimaru 1978, p. 169):

$$I(\vec{r},\hat{s}) = \frac{dP}{\cos\theta\, da\, d\omega\, dv} \tag{1}$$

in which θ is the angle between the vectors $\hat{s}$ and $\hat{s}_0$ and dP is the power flowing in a differential solid angle $d\omega$ and in a differential frequency bandwidth dv. Specific intensity thus has the dimensions of $\mathrm{W\,m^{-2}\,sr^{-1}\,Hz^{-1}}$, and has a constant value along a straight ray line in free space. By contrast with conventional power density (measured in $\mathrm{W\,m^{-2}}$), which follows an inverse-square law with increasing distance, the constant value of specific intensity along a ray line is due to the solid-angle differential $d\omega$ in the denominator. As distance from the source increases, the power contained in a constant solid angle remains constant, and so does specific intensity. This useful property underlies the equations of radiative transport theory, which are based on balancing energy into, out of, and through a ray path in a medium which may contain a gas, plasma, or particles that can absorb, emit, and scatter radiation.

Fig. 2 illustrates some important dimensional parameters of the problem of determining the visual appearance of ball lightning. Consider a BL object whose boundary is defined by a sphere of

Fig. 1. Candle flame photographed in darkness (left) and in bright incandescent light (right). *Note*: Exposure and brightness/contrast adjusted to simulate typical visual experience.

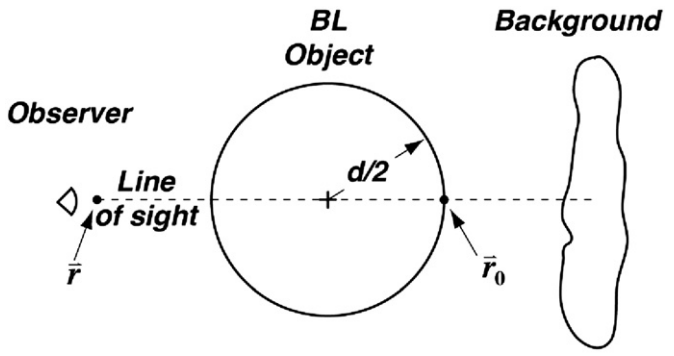

Fig. 2. Observer at location $\vec{r}$, BL object with diameter d, and background along line of sight with origin of coordinate system in background.

diameter d. Outside the sphere is air at standard temperature and pressure. Inside the sphere is a gas or plasma containing particles, all of which can scatter, absorb, or radiate energy. In the absence of a specific theory regarding the internal structure of the BL object, we will assume it is homogeneous and isotropic, although this is undoubtedly an oversimplification. Fortunately, most of the results of the following analysis depend only on the integrated absorption or scattering through the volume of the object, so they will still apply if it is found that the interior structure of BL objects is more complex than that assumed here.

We also allow for the gas or plasma inside the sphere to radiate both line and continuum spectra, even in the absence of particles.

A line of sight originates with the background, goes through the BL object's center, and terminates in the observer's eye. For the purposes of this analysis, the observer will be assumed to have normal vision adapted to the prevailing level of background illumination that was present before the appearance of the BL object. The total specific intensity I_0 received by the observer's eye along the designated line of sight is composed of two parts: the reduced incident specific intensity I_{ri}, which consists of background radiation reduced by any absorption or scattering in the BL object; and a diffuse specific intensity I_d due to light that is either emitted directly to the eye by the object, or scattered into the line of sight from other sources.

The reduced incident specific intensity I_{ri} is related to the incident specific intensity I_i coming from the background and illuminating the back of the BL object by the expression

$$I_{ri}(\vec{r},\hat{s}) = I_i(\vec{r}_0,\hat{s})\exp\left(-\int_0^s \rho(s')\sigma_t(s')ds'\right) \tag{2}$$

The upper limit of integration s is distance along the line of sight from the point of background-light entry $\vec{r}_0$ at the rear of the BL object, to the point $\vec{r}$ at which the radiation is being observed. The function $\rho(s')$ is the number density of particles (m^{-3}) along the ray path, and σ_t is the total extinction cross section (m^2) of each particle. The dimensionless integral in Eq. (2) is termed τ, the *optical distance*. If the particular path shown in Fig. 2 has a constant number density of uniform particles along the section inside the sphere, each of which has the same extinction cross section, the integral in Eq. (2) reduces to the expression

$$\tau = \rho\sigma_t d \tag{3}$$

assuming scattering and absorption occur only inside the sphere.

The diffuse specific intensity I_d itself is made up of two contributions: light from the surrounding sources scattered into the ray, and light emitted directly from the particles and gas in the BL object. For most BL objects of interest, most of the light available for scattering into the beam is generated within the object itself, so background radiation will be neglected in the calculation of I_d. Another simplifying assumption we will make is that within the object, the internally generated light intensity available for scattering into the beam is isotropic. While this assumption is technically incorrect because vectors in different directions traverse different amounts of radiating material and thus produce varying amounts of light, especially near the surface of the sphere, it will allow considerable simplification of the expression for I_d.

The general expression for diffuse specific intensity I_d is (Ishimaru, 1978)

$$I_d(\vec{r},\hat{s}) = \int_0^s \exp[-(\tau-\tau_1)]\left[\left(\frac{\rho\sigma_t}{4\pi}\right)\int_{4\pi sr} p(\hat{s},\hat{s}')I(\vec{r}_1,\hat{s}')d\omega' + \varepsilon(\vec{r}_1,\hat{s})\right]ds_1. \tag{4}$$

The variable τ is the optical length along the line of sight from zero to the limit of integration s, which is also the distance from the point where the background radiation enters the sphere to the point of observation. The variable τ_1 is the optical length from zero to the *variable of integration* s_1. The leading exponential in this case is simply a weighting factor that accounts for the subsequent absorption and scattering of any light that is emitted or scattered into the ray at a given point inside the sphere.

Because light can be scattered into the beam from any angle, the second integral over 4π steradians is needed to account for contributions from all angles. The function $p(\hat{s},\hat{s}')$ is called the *phase function* (an astronomical term relating to lunar phase, not electromagnetic phase), and is related to the albedo W_0 of a single particle by the expression (Ishimaru, 1978)

$$\frac{1}{4\pi}\int_{4\pi sr} p(\hat{s},\hat{s}')d\omega = W_0 \tag{5}$$

Albedo, of course, is the ratio of scattering cross section σ_s to total extinction cross-section σ_t.

The emission term $\varepsilon(\vec{r}_1,\hat{s})$ has the dimensions W sr^{-1} m^{-3} and is in general a function both of position $\vec{r}_1$ and direction $\hat{s}$.

Next, we make use of the assumption that radiation into the ray is isotropic, although it may vary with distance s_1. Denoting the isotropic specific intensity inside the sphere at point $\vec{r}_1$ as $I_{sph}(\vec{r}_1)$, the integral over 4π steradians in Eq. (4) becomes a product:

$$\int_{4\pi sr} p(\hat{s},\hat{s}')I_{sph}(\vec{r}_1)d\omega' = 4\pi W_0 I_{sph}(\vec{r}_1) \tag{6}$$

If the emission from both particles and gas is also isotropic and constant within the sphere, we can then combine the simplified version of Eq. (4) with Eqs. (2) and (3) to obtain a simplified expression for the total specific intensity at the eye:

$$I_0 \approx I_i\exp(-\rho\sigma_t d) + [1-\exp(-\rho\sigma_t d)]\left(W_0 I_{sph} + \frac{\varepsilon}{\rho\sigma_t}\right) \tag{7}$$

With the stated assumptions, this expression allows the calculation and comparison of all contributions to the total specific intensity: reduced emission from the background through the object to the eye, scattering into the beam, and direct emission from particles, gas, or plasma within the beam. As the following section will show, the criterion of apparent opacity places a constraint upon the ratio of I_{ri} (the light from the background that comes through the object to the observer) to I_d (the light emitted from the object), and this constraint arises from the manner in which the normal eye perceives contrast.

3. Limits of observable contrast

The literature on how the eye perceives contrast is vast, and no attempt will be made to review it here. Instead, we will cite specific results from this field which will enable us to specify

what criteria must be met in order for a glowing sphere to appear opaque when in front of a given background with a specific illumination level. Then we will use these criteria to establish constraints on the parameters that appear in Eq. (7) above.

Physiological experiments undertaken by Van Nes and Bouman (1967) in the 1960s established the relationship between the minimum perceptible contrast between light and dark areas in a field of view, and the general level of illumination. Measurements of perceived brightness are expressed in photometric rather than radiometric units, partly because the human eye is not equally sensitive to all visible wavelengths. The relationship between the two systems of units is established by the definition of the base unit of photometry, the *candela*, in terms of radiant power. The candela is "the luminous intensity, in a given direction, of a source which is emitting monochromatic radiant energy of frequency 540×10^{12} Hz and whose radiant intensity in that direction is 1/683 W sr^{-1}" (Wyszecki and Stiles, 1982, p. 255). To evaluate the photometric unit of luminous flux F_L from a given source whose spectral radiant-power output is expressed as $P(\lambda)$ (in W nm^{-1}), it is necessary to perform an integration of the output power over wavelength as weighted by the *photopic luminous efficiency function* $V(\lambda)$ (Wyszecki and Stiles, 1982, p. 787):

$$F_L = K_m \int_\lambda P(\lambda)V(\lambda)d\lambda \tag{8}$$

The unit of luminous flux is the *lumen*. The term $V(\lambda)$ is a dimensionless luminous efficiency function having a maximum value of 1.0 at a wavelength corresponding to 540×10^{12} Hz, and the constant $K_m=683$ lm W^{-1}. The Commission Internationale de l'Eclairage (CIE) established the function $V(\lambda)$ as part of the CIE 1931 Standard Colorimetric System to represent the sensitivity of the normal eye in photopic conditions, in which the level of illumination is high enough so that the eye's color-sensitive cones are active as well as the low-light-sensing rods. When a given luminous flux F_L (in lumens) is uniformly incident on a surface area A (in m^2), the area is said to receive an *illuminance* $E=F_L/A$. The unit of illuminance is the lux, which therefore has the dimensions of lm m^{-2}.

Clearly, in order to evaluate the luminous intensity of a given light source in lumens, the source's spectrum must be known or estimated, although the luminous efficiency function is smooth enough so that low-resolution spectral measurements with two or three filters can often be sufficient to determine the luminous intensity of a source with reasonable accuracy. In particular, the emissions of perfect black-body radiators have precisely known spectral intensities, and can be expressed readily in terms of luminous intensity without recourse to experiments.

Researchers who report results relating to the visual characteristics of the eye often express the intensity of the optical stimulus in terms of a unit called the troland. The *photopic* troland (t) is defined as the product of photopic *luminance* L (in candelas per square meter) and the area of the pupil of the eye p (in square millimeters). The normal pupil in average room light is about 3 mm in diameter, which is a pupil area of $p_0=7.07$ mm^2. We will assume this area for all conversions of trolands to luminance (in candelas m^{-2}).

Suppose a given situation produces a specific intensity function $I_0(\nu)$ at the point of observation. To convert this intensity into trolands, one must first make the transition from radiometric to photometric units. An added complication is the fact that specific intensity has the dimensions of W m^{-2} sr^{-1} Hz^{-1}, while the photometric unit of luminance L is specified in terms of an integration with respect to wavelength, not frequency. If c' is the speed of light in the (uniform) medium under consideration, $I(\nu)$ is a specific intensity function, and λ is the wavelength, the luminance of a ray having the given specific intensity function, whose significant energy content lies between the wavelength limits λ_1 and λ_2, is

$$L = K_m c' \int_{\lambda_1}^{\lambda_2} \frac{I(c'/\lambda)d\lambda}{\lambda^2} \tag{9}$$

Given the luminance L and a pupil area p in mm^2, the resulting retinal illumination in trolands is simply the product Lp.

Turning to the question of contrast, there are several definitions of visual contrast in use, but the one employed by Van Nes and Bouman (1967) is the "Michelson contrast" in which contrast or modulation M is defined by the ratio

$$M \equiv \frac{L_{\max}-L_{\min}}{L_{\max}+L_{\min}} \tag{10}$$

in which $L_{\max}$ and $L_{\min}$ are the maximum and minimum levels of luminance, respectively, in the field of view. In a series of experiments with a human subject, Van Nes and Bouman examined the threshold at which increasing levels of contrast become barely perceptible with respect to two variables: the average illumination level in trolands, and the spatial frequency of the sinusoidal contrast target in terms of cycles per degree of view. As one might expect, higher levels of illumination permitted the perception of smaller levels of contrast, and the illumination level also influenced the spatial frequency at which the threshold was lowest.

The salient results of the Van Nes experiments (Van Nes and Bouman, 1967) are that at low light levels, fine detail (high spatial frequency) cannot be detected as well as coarser features that are larger than the minimum spatial-frequency range of the study (<0.5 cycles/degree). But at a spatial frequency of 0.5 cycles/degree, targets with a contrast modulation of 12% are at the threshold of discernability with the minimum level of illumination studied, which was 9×10^{-4} trolands. At higher levels of illumination, the maximum sensitivity to contrast occurs at smaller levels of detail (higher spatial frequency), and the threshold eventually plateaus with high light levels (>90 trolands) at a modulation of about 0.2%.

As we will show below, for typical BL luminance levels, the retinal illumination will be well above 90 trolands. Therefore, for the purposes of this study we can assume that any contrast (modulation) greater than $M=0.2\%$ will be visible, meaning that the BL object will no longer appear opaque for apparent contrast levels greater than a modulation of 0.2%.

For the purposes of this evaluation, certain factors will be assigned a nominal or typical value. One such factor is the assumed contrast of the background. A perfectly uniform background with modulation of 0%, such as a uniformly gray cloudy sky, would make it very difficult to determine whether a BL object was opaque or transparent, because there would be no contrasting features of the background to be seen through the object. On the other hand, one cannot assume that a BL object will pose obligingly before a test pattern of 100%-modulated black and white bars, for example. A reasonable course to pursue is to assume a medium-contrast background with a modulation M_B of 50%, which implies that the contrast ratio of maximum background luminance to minimum background luminance $R_C=L_{\max}/L_{\min}=3$. We further assume that the average background reflectivity ε is 0.5, which implies that the more reflective areas have a reflectivity of 0.75 and the less reflective ones, 0.25. Finally, we will assume a wide spectrum of spatial frequencies present in the background scene, so that there are some spatial frequencies near the optimum value (about 4 cycles/degree) for contrast discrimination at the prevailing light level of 90 trolands or more.

Let the luminance due to emission and scattering into the line of sight by the BL object be denoted L_d. If the luminance due to the light emitted from the background as reduced by passage through

the BL object is denoted as L_{ir}, we need to express luminance from both the light and the dark areas of the background. Let the reduced luminance from the light areas be L_{ir}^{+} and from the dark areas be L_{ir}^{-}. Because all radiation from the background is presumably attenuated equally (we will neglect any wavelength dependence of scattering or absorption in the object), the background luminance contrast ratio in terms of maximum-to-minimum luminance will be the same for light entering and exiting the object: namely, $L_{ir}^{+}/{}^{-}L_{ir}^{-}=L_{\max}/L_{\min}=R_C$. Ignoring any issues relating to wavelength dependence, the total luminance received by the eye of the observer is the sum of the reduced luminance L_{ir} from the background and the diffuse luminance L_d, which is due to emission from the BL object and from light scattered into the line of sight inside the object. When the line of sight includes a light portion of the background, the total luminance will be $L_d+L_{ir}^{+}$, and if it includes instead a dark portion of the background the total will be $L_d+L_{ir}^{-}$. This also assumes that the BL object itself has no features of its own to interfere with visualization of the background. If these assumptions are made, the modulation visible to the observer looking through the BL object at the background is therefore

$$M_0=\frac{(L_{ri}^{+}+L_d)-(L_{ri}^{-}+L_d)}{(L_{ri}^{+}+L_d)+(L_{ri}^{-}+L_d)}=\frac{L_{ri}^{+}-L_{ri}^{-}}{L_{ri}^{+}+L_{ri}^{-}+2L_d} \tag{11}$$

If we denote the extinction ratio of incident background luminance to reduced background luminance as $L_{ir}/L_i=\alpha$, and divide through by the minimum background luminance L_{Bmin}, we obtain

$$M_0=\frac{\alpha(R_C-1)}{\alpha(R_C+1)+2(L_d/L_{\mathrm{Bmin}})} \tag{12}$$

For a constant background-light attenuation factor α and a constant background contrast ratio R_C, there is thus a direct correspondence between the observed contrast M_0 and the ratio of diffuse luminance (primarily BL emissions) to minimum background luminance, which we will denote as $L_d/L_{\mathrm{Bmin}}=\beta$. If the observed contrast M_0 exceeds the threshold for visibility as specified in the Van Nes data for the prevailing level of luminance, the background contrast can be seen through the BL object, and the object no longer appears opaque. Based on the various records of sightings, the variation in BL luminance is unlikely to cover a range much larger than a factor of 100 or so. This will further restrict the parameter space in which the properties of BL must produce the effects observed, as we show below.

In the next three sections, we will examine three distinct possible mechanisms for BL luminosity: a plasma-only model, a particle-only model, and a fractal-cluster model. These models are not intended to simulate actual BL in a realistic way, but to show how each mechanism in its "pure" form could account for the luminosity of BL observed by witnesses. It is likely that the true mechanism of BL is a mixture of two or more of these models, at a minimum. Also, all these models assume a quasi-stable situation in which the luminous part of the BL structure is homogeneous and the luminosity-producing mechanisms do not change much with time over the period of observation.

In (Amirov and Bychkov, 1994), it was shown that through an ANOVA study involving about 1750 eyewitness BL reports that the way a BL object ends its existence is correlated with its size and lifetime. They divided their cases into "exploding" and "decaying" objects, depending on whether the object terminated with a violent abrupt explosion, or whether it simply silently faded away and became invisible. They concluded that the decaying type's energy-loss mechanism was primarily through radiation only. Our assumption that the internal conditions do not change much over the BL object's lifetime is more likely to be correct with the decaying type of BL. It is possible that more complex models than those presented here are needed to account for phenomena associated with the exploding type of BL (see for example (Bychkov, 2010)).

4. Plasma-only (totally non-absorbing and non-scattering) BL object

One extreme case concerning the optical nature of a BL object is that it is totally transparent (in the radiometric sense, not the visual sense) to all visible wavelengths, and its optical activity consists solely of line or continuum emission from gas or plasma only (no particulates). A commonplace realization of this phenomenon is the appearance of a clear (not phospor-coated) "neon sign" luminous-tube display. Such a tube appears opaque in a dim room simply because dimly lit objects behind it cannot reflect enough light to provide the minimum contrast level needed to be discerned, when the light emitted from the tube itself is added. The extinction coefficient α in Eq. (12) becomes unity for such an object, and with our assumption of a nominal contrast ratio R_C value of 3, we obtain the following special case for observed contrast M_{0C} through a non-absorbing and non-scattering BL object:

$$M_{0C}=\frac{1(3-1)}{1(3+1)+2\beta}=\frac{1}{2+\beta} \tag{13}$$

The question we will address is: under what minimum level of background illumination $E_{\min}$ (in lux=lumens m^{-2}, abbreviated lx) will a BL object appear opaque when superimposed against a background with a modulation (contrast) $M_B=50\%$? We will assume that the background scatters light uniformly into a half-sphere (2π radians). (Although the usual procedure is to assume a Lambertian surface whose light intensity depends on the cosine of the angle from normal, the actual angle is unknown and an assumption of isotropic scattering makes for easier calculations.).

We will begin by taking at their word numerous observers who say that the brightness of the BL object was comparable to that of an incandescent lamp with a primary input power of between 20 and 200 W. As noted above, most such comparisons fall between these two extremes. The typical luminous efficacy of a frosted incandescent lamp is about 14 lm W^{-1} (Wyszecki and Stiles, 1982). The range of 20 to 200 W therefore corresponds roughly to a range in total emitted luminous flux F_{OBJ} of $(20\times 14)=280$ to $(200\times 14)=2800$ lm. Further assuming that the light from the BL object is emitted uniformly over an apparent disc of diameter d meters, as viewed by a distant observer, the luminance L_d from the object is the total luminous flux (lumens) divided by the product of the total solid angle (4π, assuming isotropic emission) and the apparent projected area:

$$L_d=\frac{F_{OBJ}}{4\pi(\pi d^2/4)}=\frac{F_{OBJ}}{(\pi d)^2} \tag{14}$$

The coefficient β is defined as the luminance L_d of the BL object divided by the minimum luminance of the background, L_{Bmin}. The latter distance-independent quantity can be calculated using the background assumptions made in the previous paragraph:

$$L_{\mathrm{Bmin}}=\frac{E_{\min}\varepsilon_{\min}}{2\pi\ sr}=K_{EL}E_{\min} \tag{15}$$

in which the conversion factor $K_{EL}=39.79\times 10^{-3}\ \mathrm{sr}^{-1}$. The units of $E_{\min}$ are lux (lumens per square meter) as explained above.

The dominant illumination of concern in visual perception of a BL object is the luminance of the object itself. Assuming a typical BL object diameter of $d=25$ cm, Eq. (14) gives a luminance range of 453.9 to 4539 cd m^{-2} for the assumed total luminosities of 280 to 2800 lm, respectively. Converting these levels to trolands using the assumed typical pupil diameter of 3 mm, we find that the

typical retinal illumination from this range of luminosities is 3210 to 32,100 trolands. This is well above the level of illumination of 90 trolands which causes the minimum perceptible contrast modulation to fall to a plateau of about $M_{0C}=0.2\%$, as mentioned above. Therefore, to find the illumination necessary for a background of typical contrast to show through a BL object which neither scatters nor absorbs radiation, we simply need to solve Eqs. (13) and (15) for the minimum background illumination range for $E_{\min}$, given the range of values for L_{OBJ}:

$$E_{\min}=\frac{L_{OBJ}}{K_{EL}(1/M_{0C}-2)} \tag{16}$$

Solving this equation for the two cases of the 20-W and 200-W extremes, we find that the background illumination level for barely making a typical-contrast background visible through the object ranges between 22.9 and 229 lx. What does this range imply for actual observational circumstances?

The lighting inside a typical residence is in the range of 50 to 80 lx, while an outdoor surface on a very overcast day may receive an illumination level of 100 lx or more. So we find that unless the background is illuminated to a level brighter than either an overcast day or a relatively dim interior, the BL object is likely to appear opaque. Of course, if the background is darker or of lower contrast than our assumed typical values for reflectance and contrast, an even higher background lighting level will be needed to cause the background to be barely visible through the BL object. And high-contrast features on the BL object itself (brighter areas, sparks, etc.) may mask the appearance of a low-contrast background, so these factors would also require a higher illumination level of the background for a BL object to appear translucent than this minimum estimate indicates.

The conclusion of these calculations for an assumed completely non-absorbing and non-scattering BL object, is that in light levels of less than about 20 lx (darker than a poorly-lit interior), such a BL object with typical light emission levels will appear to be opaque for the same reason a candle in a dark room appears opaque: the light emitted from the object overwhelms the light transmitted through the object from the background. Any sightings at night or in darkened interiors will fall into this category. On the other hand, if an eyewitnesses report implies that the background illumination was much brighter than this (such as outside on a cloudy or sunny day, or a brightly lit interior), and also explicitly states that the BL object of typical brightness appeared opaque, it is unlikely that the BL object was non-absorbing and non-scattering, for the reasons stated above.

Because most BL reports do not explicitly mention opacity or transparency, this conclusion has little traction on its own with regard to elucidating new information about ball lightning. However, when we combine it with subsequent calculations regarding the optical activity of any particulates which may contribute to light emission from BL, the picture becomes more informative.

5. BL with emission from individual particulates only

Turning from the assumption of light emission from gas or plasma only, we now assume another extreme hypothetical case: a BL object whose light emission comes solely from particles that are too large to be termed molecules, but too small to fall out of suspension in air in a short time. This includes larger nanoparticles, dust particles, and similar objects in the range of about 50 to 100 nm in diameter. This range of sizes is typical of smoke and other particulates which are small enough to be suspended in air for the typical lifetime of a BL object. These particles are assumed to form an aerosol suspended in ordinary air, and are heated to a uniform temperature T_P by an unstated mechanism. Possibilities for heating range from combustion (see e.g., Abrahamson, 2000, 2002b) to ion or electron bombardment, but consideration of the nature of the heating mechanism in detail is beyond the scope of this paper. In this section, we are concerned only with particle characteristics that are relevant to our accounting for the luminance and color of BL objects reported by eyewitnesses.

In what follows, we will use carbon particles as a working model, not because we think BL is likely to contain large quantities of carbon, which would quickly disappear in an oxidizing atmosphere anyway, but because the optical absorption and scattering behavior of small carbon particles has been the subject of intense investigation and is reasonably well understood. In particular, carbon particles or aggregates can closely approach the ideal black-body radiator that we assume for the following simplified analysis.

Particles are characterized in radiative transport theory by means of their cross-sections for absorption (σ_a) and scattering (σ_s), which add up to the total extinction cross-section σ_t:

$$\sigma_t=\sigma_a+\sigma_s \tag{17}$$

We can temporarily eliminate scattering from consideration by assuming that the particles are ideal black-body absorbers which have a negligible scattering cross-section, so that the total scattering cross-section equals the absorption cross-section: $\sigma_t=\sigma_a$. This amounts to setting the albedo W_0 to zero. We will further assume that the particles are also perfect black-body emitters having the maximum theoretical emissivity possible for their size and temperature. E. M. Purcell showed that an ideal emissivity of 1.0 is sometimes impossible for particles smaller than a certain size, depending on the particle's temperature (Purcell, 1969). Purcell found that the maximum theoretical emissivity of spherical particles of radius r at a temperature T is the lesser of unity or $8948rT$, where r is in meters and T is in K. This means that the maximum emissivity of a 50-nm-radius sphere at 1100 K is only 0.49, not 1.0, and less at lower temperatures. This limitation does not alter the fact that particles in this size range are still Rayleigh scatterers for light of visible wavelengths ($\sim$400–700 nm), so their scattering cross-section is still negligible compared to their absorption cross-section. Whatever the size and emissivity of the individual particles, one can always assume in the following derivation, if necessary, that the optical path length is great enough to absorb incoming radiation completely, making the BL object as a whole a perfect black-body radiator, even if its constituent particles are not.

Kirchoff's law of thermal radiation ensures that at a given wavelength, a perfect absorber of radiation is also a perfect (black-body) emitter. Therefore, a BL object that is sufficiently optically dense to absorb all incident light will behave as an ideal black-body radiator, and Planck's radiation law gives the radiance (specific intensity) directly as

$$I_{BB}(\nu,T)=\frac{2h\nu^3}{c^2}\frac{1}{\exp(h\nu/\lambda k_BT)-1} \tag{18}$$

in which h=Planck's constant (6.626×10^{-34} J s^{-1}), c is the speed of light, and k_B=Boltzmann's constant (1.38×10^{-23} J K^{-1}). Because the specific intensity I_{BB} as a function of frequency (or wavelength) is known for an ideal black body, its luminance is easily calculated from its temperature. We will denote the known luminance function of a black body of temperature T (K) as $L_{BB}(T)$, measured in candelas per square meter.

The luminance function can be obtained through a straightforward integration of Eq. (18) in a conversion integral analogous to the power-to-luminous-flux conversion integral of Eq. (8), in which the radiance is weighted according to the photopic luminous efficiency function $V(\lambda)$. The function $L_{BB}(T)$ is presented

graphically in Wyszecki and Stiles (Wyszecki, 1982, p. 29) and can be approximated with better than 2% accuracy over the temperature range of 1100–3500 K with a fourth-order polynomial in T normalized to 2000 K. We used such a polynomial approximation in the following calculations.

Strictly speaking, the discussion in the preceding paragraphs applies only to an object that is optically thick enough so that the optical distance $\tau=\rho\sigma_a d$ reduces the exponential term in Eq. (7) to a negligible value. For example, an optical distance of $\tau=5$ would produce an object whose behavior approximates that of an ideal black-body radiator to within 1%. However, the more typical case with BL objects may be that the optical distance is considerably smaller, so we must also consider cases in which the BL object is optically thin. A thermodynamic argument can yield a simple expression for the radiance and luminance of a BL object whose radiation originates with black-body particles and whose optical distance is any arbitrary value from zero up to infinity.

Suppose a BL object emitting light only from ideal black-body particles within it is interposed between the observer and an ideal black-body background, and both background and BL particles are at a temperature T_0. The total specific intensity received by the observer (integrated over all wavelengths) will of course be $I_{BB}(T_0)$, but this intensity is composed of two parts: (1) radiation from the background reduced by absorption in the BL object, and (2) radiation from the BL object itself. These parts correspond to the two terms in the following equation, which is a specific case of Eq. (7):

$$I_{BB}(T_0)=I_{BB}(T_0)\exp(-\tau)+(1-\exp(-\tau))\left(\frac{\varepsilon(T_0)}{\rho\sigma_a}\right) \tag{19}$$

In Eq. (19) we have dropped the scattering part of the second term because of the earlier assumption of zero scattering cross-section. Eq. (19) immediately yields

$$\varepsilon(T_0)=\rho\sigma_a I_{BB}(T_0) \tag{20}$$

which gives the emissivity term in Eq. (7) as a function of particle number density ρ, particle absorption cross-section σ_a, and black-body specific intensity $I_{BB}(T_0)$.

We now relax the restriction that both the BL object and the background must be at the same temperature T_0. Assuming linearity, the total specific intensity I_0 observed through a BL object whose particles are at a temperature T_P which differs from the background temperature T_B is thus

$$I_0=I_{BB}(T_B)\exp(-\tau)+(1-\exp(-\tau))I_{BB}(T_P) \tag{21}$$

In the typical case for which the BL object appears opaque, any radiation received from a room-temperature background is negligible compared to the direct radiation from the object itself, and so we will neglect the first term in Eq. (21). This allows us to approximate the specific intensity of the black-body-particle BL object as

$$I_{d(BBBL)}\approx(1-\exp(-\tau))I_{BB}(T_P) \tag{22}$$

which gives the BL object's specific intensity as a function of optical length τ and particle temperature T_P.

For a constant color distribution, which in the case of Planck-law radiation means a constant source temperature T_P, luminance is directly proportional to specific intensity. Therefore, Eq. (22) allows us to substitute the luminance function $L_{BB}(T_P)$ for the specific intensity function $I_{BB}(T_P)$, yielding the luminance $L_{d(BBBL)}$ of a BL object consisting of ideal black-body radiating particles as the sole source of illumination:

$$L_{d(BBBL)}\approx(1-\exp(-\tau))L_{BB}(T_P) \tag{23}$$

While Eq. (23) is instructive, it depends on knowledge of optical distance τ, which in turn requires information about the number density and absorption cross-section of the assumed particles. Fortunately for this study, the absorption and scattering cross-sections of carbon particles have properties that approximate the hypothetical black-body ideal, and have been studied extensively in connection with atmospheric pollution investigations and related phenomena. We will rely on one such study (Schnaiter et al., 2006) to provide us with actual scattering and absorption cross-sections that will allow a realistic calculation of how dense and hot particles must be in order to account for the typical luminosity of BL objects.

As shown above, the typical luminance of BL objects is estimated to lie between about 454 to 4540 cd m^{-2}. Eq. (23) shows that an infinite number of combinations of optical distance τ and intrinsic particle luminance $L_{BB}(T)$ can yield the same observed luminance $L_{d(BBBL)}$. That is, a given observed luminance can be produced either by an optically thin BL object with very hot particles, or an optically thick BL object with cooler particles.

An additional constraint is imposed by the observed color ranges of BL objects. Although almost every color in the spectrum has been reported at least a few times, the preponderance of observers report colors in the range of red through yellow to white. This range matches the colors produced by an ideal black body as its temperature is raised from about 1100 K, where optical emission becomes barely visible in the red portion of the spectrum, to 3500 K, which produces a yellowish-white of extreme brilliance. Because carbon sublimes at about 3900 K and is probably one of the most refractory materials likely to be found in BL objects, we have limited the modeled range of temperatures to between 1100 and 3500 K.

First, assume that a hypothetical BL object is optically thick enough to act as an ideal black body. In that case, the exponential term in Eq. (23) vanishes and the luminance of the BL object is equivalent to the luminance of a black body. By solving Eq. (23) for temperature T, we can find the temperatures that would produce the observed luminances of 454 to 4540 cd m^{-2}, (or 45.4×10^{-3} to 0.454 cd cm^{-2}, to use units more commonly employed in photometry). These correspond to a black-body temperature range of approximately 1270 to 1451 K. From a color standpoint, these temperatures are in the deep red range. While it is possible that some red BL objects may therefore be optically thick enough to act as black bodies, this simple model fails for colors that correspond to higher temperatures, because the (hypothetically black-body) object would be much brighter than the typical eyewitness describes. For example, because luminance rises almost exponentially with temperature, a black-body BL object at 2000 K still has an orange–red color, but shows a luminance of about 45 cd cm^{-2}, almost a hundred times brighter than the brightest (200-watt-bulb-equivalent) luminance estimates of most BL eyewitnesses.

If we allow for optically thin BL objects, the emitting particles may be hotter than those in the hypothetical optically-thick object and still produce a total light emission and luminance that is consistent with eyewitness observations. Examining a range of optical distances that vary from about $\tau=4\times10^{-5}$ to $\tau=5$, we find that the required temperatures to give the observed estimated luminances range between 1100 and 3500 K, which is in the range of reasonable temperatures for incandescent light emission. The gray band in Fig. 3 shows the range of temperatures required to produce luminances equivalent to the output of incandescent lamps in the 20-W to 200-W range, as a function of the BL object's optical distance τ. The figure shows that as the BL object becomes optically thinner (smaller τ), the ideal black-body particles must become hotter in order to keep the BL object's luminance within the estimated range of 45.4×10^{-3} to 0.454 cd cm^{-2}.

The data in Fig. 3 have several interesting implications. First, by varying the BL object's optical thickness, one can produce a (hypothetical) BL object with any Planck-radiation color from

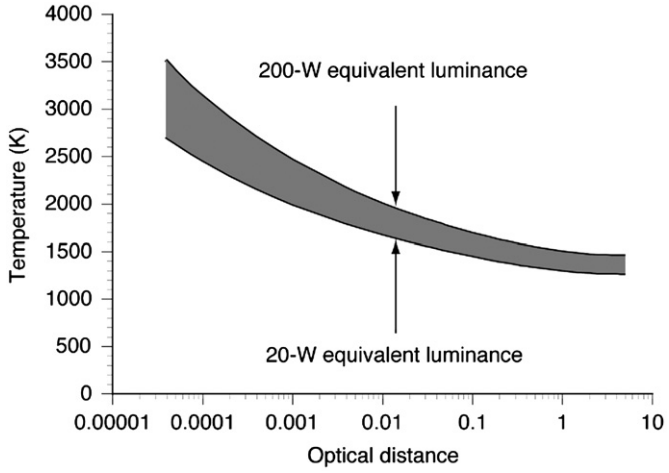

Fig. 3. Range of temperatures required for producing luminance equal to 20-W to 200-W incandescent lamp plotted as function of BL optical distance. (For interpretation of the references to color in this figure legend, the reader is referred to the web version of this article.)

deep red (~1100 K) to yellow–white (~3500 K), and still stay within the luminance range cited by many eyewitnesses. In order to do this, the optical distance must range from about 4×10^{-5} to unity or more, necessitating a logarithmic axis to display the values in one graph. This wide range is due largely to the almost exponential dependence of luminance on temperature, at least for lower temperatures.

Given the assumption of uniform particle density within the BL object and the fact that the optical distance τ is the product $\rho\sigma_a d$, the only variable that can reasonably change over such a large range is the particle number density ρ. The physical size d is one of the few BL parameters which eyewitnesses can estimate accurately to within a factor of 2 or so, and if we maintain our assumption that the particles have a physical size in the fairly narrow range of 50 to 100 nm, their absorption cross-section σ_a is limited to a rather narrow range covering at most a factor of 10, given that they are basically completely absorbing particles with an albedo of zero. (We should mention that if larger particles are allowed, it will take fewer per cm^3 to produce a given luminance level, but in order to simplify the analysis, we chose not to vary particle size.)

To employ physically reasonable numbers in an estimate of the number density of particles required to account for the observed luminance under the assumption of fully-absorbing particles, we turn to the work of Schnaiter (2006). In their investigation of the nature of carbon particulates and their role in air pollution and climate change, they produced a variety of both elemental carbon (EC) and organic carbon (OC) particles with a propane-synthetic-air flame in a controlled combustion-chamber environment. With an atomic ratio of carbon to oxygen atoms of 0.29 (a "lean" mixture with excess oxygen), their system produced a mixture of particles which they estimate were only $8.5\pm2.9\%$ organic carbon (mostly polycyclic aromatic hydrocarbons), with the remaining particles consisting of elemental carbon (soot). This mixture had an albedo ranging from 0.27 ± 0.01 at $\lambda=450$ nm down to 0.22 ± 0.01 at $\lambda=700$ nm, with a *mass* absorption cross-section $\sigma_{a(m)}=5.5\pm0.7\ m^2\ g^{-1}$ at $\lambda=550$ nm. The relationship between mass cross-section $\sigma_{a(m)}$ and cross-section per particle σ_a is

$$\sigma_a=\sigma_{a(m)}m_p \tag{24}$$

where m_p is the particle mass. Assuming a particle mass density $\rho_p=2\ g\ cm^{-2}$ (somewhat less than solid graphite) and a particle diameter of 75 nm, multiplying $\sigma_{a(m)}$ by an average estimated particle mass of 4.41×10^{-16} g yields an average particle absorption cross-section of $\sigma_a=2.4\times10^{-15}\ m^2$. This is only slightly smaller than the projected area of the (presumably spherical) particle of $4.4\times10^{-15}\ m^2$, showing that the experimentally measured particles are indeed good absorbers.

Because the measured albedo of the carbon particles in question averages 0.25, to estimate the total specific intensity from a hypothetical BL object containing such particles Eq. (7) must be used so as to include radiation scattered into the line of sight. Some simplification can be obtained from the fact that the object is almost certainly optically thin. For example, the highest number density of particles measured in the experiments described in (Schnaiter, 2006) was $2\times10^{11}\ m^{-3}$, which for a 25-cm path length d and absorption cross-section $\sigma_a=2.4\times10^{-15}\ m^2$ yields an optical length $\tau=1.2\times10^{-4}$. Using the first two terms in the power-series expansion of the exponential allows us to simplify Eq. (7) to

$$I_0\approx I_i+d(\rho\sigma_t W_0 I_{sph}+\varepsilon) \tag{25}$$

To a first approximation, the background specific intensity I_i passes unattenuated through the optically-thin sphere, while the sphere's contribution to the total specific intensity consists of a scattering term proportional to the ambient specific intensity I_{sph} within the sphere, plus a direct-radiation term ε which can be found using Planck's radiation law and the expression for ε given in Eq. (20). Making the assumption that the ambient specific intensity $I_{sph}=I_{d(BBBL)}/2$ (that is, the average ambient intensity is half of what would be seen outside the sphere), Eq. (25) becomes

$$\begin{aligned} I_0&\approx I_i+dI_{BB}(T_P)\left[\rho\sigma_a+\frac{(\rho\sigma_a)^2W_0(W_0+1)d}{2}\right]\\ &=I_i+I_{BB}(T_P)\left[\tau+\tau^2\left(\frac{W_0(W_0+1)}{2}\right)\right] \end{aligned} \tag{26}$$

Eq. (26) shows that the effect of non-zero scattering is to add a term that is second-order in τ, multiplied by a factor involving albedo W_0 which is of order unity or less. Therefore, if the optical length τ is much smaller than unity, scattering into the ray path may be neglected and the calculation is basically unaffected by a non-zero albedo, as long as the predominant effect of the particles is absorption rather than scattering. Eq. (26) also shows that this is a simplified "single-scattering" analysis. Multiple-scattering theory must be used when the typical ray is scattered multiple times, but for optically thin structures single-scattering analysis is sufficient.

A quantity of particular interest in this analysis is the number density of particles required to produce luminous intensities within the 10:1 range estimated from eyewitness observations. The fact that most BL objects whose termination is observed appear to vanish into invisibility indicates that most of them are probably optically thin, which means Eq. (26) is applicable. Taking the extreme case of high-temperature particles ($T_P=3500$ K), we can calculate the number density of particles required to produce a light in the requisite range of intensity, assuming each particle has the absorption cross-section of $\sigma_a=2.4\times10^{-15}\ m^2$ estimated from the Schnaiter data. Because the ratio of specific intensities is the same as the ratio of luminous intensities for a given temperature, the same analysis applies that was used in Eq. (23), and we find that for a BL object diameter of 25 cm, a sphere containing particles in the density range of 6475 to 64,750 cm^{-3} would produce luminous intensities in the range of 0.0454 to 0.454 cd cm^{-2}, corresponding to the observed intensities of incandescent lamps in the 20-W to 200-W range.

If the calculated particle densities fall below a certain level, one would expect the discrete nature of the individual particles to affect the appearance of the BL object. The number density of carbon particles in a candle flame, for example, is too high for the

eye to discern individual particles under normal circumstances, so the visual impression is of a continuous, uniformly bright source. Some BL observations indicate the existence of a distinguishable fine structure. For example, here are two independent observations quoted in Abrahamson (2002a):

(1). It resembled a tangle of woollen threads, as if blue threads covered a warp of red threads. The intensity of its radiation could be compared with an incandescent lamp of 120 W.
(2). The ball resembled a soft woollen tangle. It was white, bright like an incandescent lamp of 100 W to look at.

Given the eye's persistence of vision and the unfamiliar appearance of the BL objects, it is possible that rapidly moving incandescent particles might present the appearance of a "woollen tangle," although more information on the exact appearance of the objects would be needed to interpret it in terms of particle brightness and motion. Because the hottest (yellow–white 3500 K) particles would require the lowest number density to produce a luminous intensity within the observed range, objects with cooler particles would have higher number densities that would look more like a featureless smooth light source.

Moving to the opposite extreme of lower temperatures and higher number density of particles, we can assume a particle number density of $2\times10^5\,\mathrm{cm}^{-3}$ (the highest value observed in the Schnaiter paper (Schnaiter et al., 2006)). Any number density much higher than this would produce a cloud of particles so dense that it would be visible even if it were at room temperature and not emitting radiation. Although some BL observations mention seeing a whitish cloud of residual particles after the light-emitting lifetime of the BL object ends, the typical reports in which the termination of the object is observed say merely that it vanishes. This implies that the object is optically thin, at least at the end of its lifetime.

At any rate, using the assumed number density of $2\times10^5\,\mathrm{cm}^{-3}$ and an assumed object diameter $d=25$ cm, we can calculate the range of temperatures required for the production of luminosity in the range of 45.4×10^{-3} to $0.454\,\mathrm{cd\,cm}^{-2}$, corresponding to the observed apparent luminosity range of 20- to 200-W incandescent lamps. The corresponding temperature range of particles needed in a high-particle-density object to produce this luminosity range is 2408 to 3056 K. The visual colors corresponding to these temperatures are orange–red to reddish–orange, which fall well within the range of colors often cited by BL eyewitnesses. The only color in the Planck-radiator gamut which would be difficult to simulate with this model is deep red, corresponding to temperatures much below 2408 K. In order to maintain a minimum level of luminance corresponding to a 20-W incandescent lamp, the number density of primarily absorptive particles at such low temperatures would become so high that the object would eventually become optically thick (τ would no longer be much less than unity). This presents problems if the BL object is to become essentially transparent after it no longer emits light, but a very slight haze under the conditions in which many BL objects are seen may often escape notice by startled observers.

It should be emphasized that the assumption of essentially black-body radiators is probably not a realistic model for ball lightning. Even if the object's light emission is due primarily to hot particles, variations in chemical composition and particle structure can cause wide deviations from an ideal black-body radiation characteristic. For example, as Abrahamson pointed out in a theoretical study of light emission from ball lightning (Abrahamson, 2002b), a cloud of hot silicon nanoparticles at a temperature of only 1200 K would emit visible light with a spectrum that matches a 1700-K black body, that is, much closer to white than red. Given the refractive indices and dimensions of particles in a hypothetical object, one can calculate both the emission spectrum and the expected luminosity in a manner similar to that we have shown here with idealized carbon particles. However, we have shown that even an oversimplified model of near-ideal black-body-radiating particles can be adjusted to produce realistic levels of visible-light emission in a range of colors that corresponds to eyewitness observations of ball lightning.

To summarize the results of this section, the assumption that BL objects emit light solely by means of incandescent particles that are nearly ideal black-body emitters leads to a model that produces luminous intensities in the observed range (comparable to a 20- to 200-W light bulb) with reasonable particle temperatures ($\sim$2400 to 3500 K) and number densities (6475 to $2\times10^5\,\mathrm{cm}^{-3}$). This assumption also leads to colors in the range from orange-red to yellow–white, which are consistent with many observations.

As one reviewer of an early version of this article pointed out, the above analysis neglects the possibility that the particles have a lower absorption cross-section than carbon. In the limit of zero absorption, no light emission from the particles would be possible and the object would look like a cloud of smoke or fog because only scattering could occur. As the absorption cross-section is allowed to decline from an ideal black-body case, the light emission for a given temperature also declines, which means that in order to account for the observed light intensities, a higher density of particles is required for the same physical temperature, other things being equal. As we show in the next section, however, the possibility that the particles form fractal aggregates makes the light-emission process for a given mass of material more efficient, so raising the number density of particles is not the only way to achieve sufficient light emission if we assume absorption cross-sections considerably less than the theoretical maximum value.

6. Light emission from fractal aggregates only

In the last two decades a large amount of theoretical and experimental evidence has accumulated on the subject of fractal aggregates of small particles. Briefly, a fractal aggregate is a state of matter in which particles are arranged in chains and loose clusters characterized by a fractal dimension D between 1 and 3. The fractal dimension of a material can be estimated as follows: a plot of the average number of particles in a sphere of radius r versus r will show a dependence on radius that goes as r^{D-3}. By this criterion, a regular crystalline solid (counting atoms as particles) has $D=3$, and a single linear straight uniformly-spaced chain of particles has $D=1$. Most naturally occurring fractal aggregates show a value of D between 1.7 and 2.2. Fractal aggregates typically arise when a material that is normally solid at room temperature is evaporated by a high-energy event (e.g., lightning or combustion) and condenses in air from its vapor form, The resulting "diffusion-limited cluster aggregation" process makes fractal clusters in which D ranges from 1.75 to 1.9 (Sorensen, 2001), although values of D outside this range can arise from other processes.

As B. N. Smirnov points out in an early paper (Smirnov, 1993), when a given number of particles coalesce in the form of fractal aggregates, their ability to radiate, absorb, and scatter light increases compared to the same number of particles suspended independently in air. Sorensen states "The same amount of material dispersed in $D<2$ aggregates rather than compressed into compact, sphere-like clusters with $D>2$ will be much more effective at scattering and absorption" (Sorensen, 2001). This means that as a given mass of material is more porous and "fractal-like" ($D<2$) and less solid ($D\sim3$), the material will show larger scattering and

absorption cross-sections. Smirnov showed by theoretical and experimental studies of a candle flame that individual solid particles could not account for the measured data. However, when the radiation was assumed to come from fractal aggregates, each of radius $R=20$ nm and made up of particles with radius $r_0=3$ nm and a fractal dimension $D=1.9$, the inconsistency disappeared. This is because the radiated power per unit mass increases by the factor $(R/r_0)^{3-D}$ when a given mass of particles is aggregated into fractal clusters. In the same paper, Smirnov also showed how BL objects containing fractal clusters could maintain the apparent contradiction of radiating light with a spectrum consistent with a black-body radiator at several thousand K in a surrounding volume of air only a few hundred K above ambient.

The implications of fractal-cluster radiation properties for the BL theory of radiative transfer are clear. Substitution of fractal clusters for individual solid particles does not affect the main conclusions of the previous section. What is affected are the estimates for the particle and mass densities needed to account for the ranges of observed colors and intensities. While the discussion in Section 5 assumed solid particles 50–100 nm in diameter, if we substitute fractal aggregates of the same diameter range, we can achieve the same results with a much smaller mass density of material. Assuming Smirnov's fractal dimension $D=1.9$, if the assumed fractal clusters are $R=25$ nm in radius but consist of individual particles with radii $r_0=3$ nm, the volume of solid material required for the same radiant output compared to the particles in Section 5 decreases by a factor of $(r_0/R)^{3-D}=0.097$. In other words, we achieve the same radiant output as the solid-particle model in Section 5 with less than 10% of the mass. Therefore, a model which relies on fractal aggregates rather than solid independent particles for light emission requires less total mass and/or fewer individual particles than the model of Section 5 which uses individual solid particles. This has definite advantages in attempting to account for the apparent low mass and evanescent nature of low-energy BL objects, which often seem to leave no visible traces at the end of their lifetimes.

Smirnov's conclusion that fractal aggregates are more efficient at scattering and absorption than the same mass of material in isolated particles is borne out by the recent theoretical work of Liu et al. (2008) in which is shown significant increases in absorption and especially scattering compared to solid particles. And a theoretical analysis by Markel et al. (2004) of fractal aggregates of silver showed a dramatic increase in the visible-light extinction cross section, on the order of 100 or more, when individual particles were aggregated with a fractal dimension of $D=1.8$. Various laboratory simulations of ball-lightning-like phenomena such as the microwave-induced plasmoids of Dikhtyar and Jerby (2006) and the "water plasmoids" produced by pulsed DC discharges above a water surface (Egorov and Stepanov 2002; Versteegh et al., 2008) have either been shown to contain particulates that may occur in fractal form, or involve circumstances (such as evaporation of cathode material in an arc) that are known to produce fractal aggregates in other situations. And several well-known BL theories (e.g., Abrahamson, 2002b) employ fractal aggregates as an intrinsic feature of their proposed mechanisms. While detailed estimates are not possible without making rather arbitrary assumptions about the nature of the fractal aggregates, no consideration of BL light emission is complete without considering the possibility that some, if not most, of the light emitted from a BL object comes from such structures.

7. BL model with plasma, particulate, and fractal-aggregate light emission: Energy requirements

We have already mentioned the possibility that light from a BL object originates in line or continuum emissions from a plasma or plasma-like fluid. If BL objects consist of particles suspended in a plasma, they contain dusty plasmas, about which a considerable body of research has accumulated (Shukla, 2001). Without speculating as to the excitation or stabilization mechanisms which may operate in BL objects, we can make some estimates of the energy input required to produce the visible light emission noted in eyewitness accounts.

The likely luminous efficacy of a BL object in terms of lumens per watt depends on the assumed mechanism by which energy is converted into light. If a plasma-type discharge with no suspended particles is assumed, the luminous efficacy probably is in the range of 10–30 lm W^{-1}, because an unmodified "neon-sign" tube produces about 10 lm W^{-1} and a fluorescent lamp can produce 50 lm W^{-1} or more, but only with the aid of a fluorescent coating that converts invisible UV radiation into visible light. To produce a luminous intensity equivalent to a 200-W incandescent lamp, a BL object with a luminous efficacy of 10 lm W^{-1} would require a power input of 280 W (again assuming a typical incandescent efficacy of 14 lm W^{-1}). Assuming a higher luminous efficacy of 30 lm W^{-1} and an observed luminous intensity on the low end of the range (equivalent to a 20-W incandescent lamp), the power required is only 9.3 W. So if light emission is solely due to plasma line or continuum emission, the minimum power level (electrical, chemical, or otherwise) required to account for the observed luminous intensity of most observations turns out to be roughly the same as the observers' estimates of equivalent incandescent-lamp power requirements: 9.3 to 280 W.

Estimating the power required to sustain incandescence of small particles is a more complex matter. The energy loss from a small particle takes place primarily through radiation and convection, unless the particle is so hot that substantial evaporation takes place (which we will neglect). Again assuming that each particle is an ideal black-body radiator, we can estimate the power P_P radiated per particle as a function of temperature through the use of the Stefan–Boltzmann equation:

$$P_P = A_P \sigma_{S-B} T_P^4 \tag{27}$$

in which A_P is the area of the particle and σ_{S-B} is the Stefan–Boltzmann constant (5.67×10^{-8} W m^{-2} K^{-4}).

As in the earlier examples, we can examine two extreme cases. The first extreme would be a yellow–white object consisting of particles with a temperature $T_P=3500$ K and a low number density of 6475 cm^{-3}. Using the same particle diameter of 75 nm that was assumed above, a simple calculation involving the power radiated per particle, the number density of particles, and the volume of a 25-cm sphere shows that the total radiated power (not just in the visible wavelength range, but at all wavelengths) is on the order of 8 W. Because luminous efficacy of an incandescent source increases with increasing temperature, we expect this to be close to the minimum required power to account for visible BL radiation, if the intermediary medium consists of incandescent particles.

Considering the opposite extreme of a fairly dense particulate cloud (2×10^5 cm^{-3}) of cooler particles ($T_P=2400$ K), a similar calculation yields a radiated power of 54.4 W, again at all wavelengths (not only visible light). Both of these estimates produce a luminous intensity on the low end of the observed range, equivalent to a 20-W incandescent bulb, and can be multiplied by 10 to yield the power required for a 200-W-lamp equivalent source.

If the radiation is assumed to come from fractal aggregates rather than solid particles, it is difficult to quantify the difference this will make to these estimates without obtaining more details on the wavelength dependence of absorption for such aggregates. It is possible that their greater radiating efficiency will allow less total input power than estimated above to produce the same

luminous output, but without more details on the nature of the aggregates, we cannot make quantitative estimates.

The result of these estimates is that whether the light-production mechanism is purely plasma excitation, purely due to incandescent particles, or a mixture of the two mechanisms, we still come up with a total minimum required power to account for observed light emission in the range of 10–500 W.

In these estimates we have neglected any energy loss due to convection or other mechanisms that dissipate power in ways other than by emission of visible radiation. If convection is present, it must have a relatively small effect because of the observed motion of most BL objects. As pointed out by (Rakov and Uman, 2003) in the quotation above, BL objects do not typically rise as a hot convecting gas would do. If a BL object does not rise as a heated gas occupying the same volume would do, there are a limited number of possibilities as to why the object exhibits other types of motion:

(1). The visible object's average mass density *is* in fact less than that of the ambient air, but another unknown force dominates the relatively small buoyancy force in determining the BL object's net motion.
(2). The visible object's average mass density is close enough to the density of ambient air that buoyancy is no longer the dominant force on the object, and other smaller forces (wind, multipolar electrostatic or magnetic forces, etc.) are able to dictate the object's motion.

Assuming a typical mass density for sea-level room-temperature air of 1.2 kg m^{-3}, the largest buoyancy force possible on a totally evacuated 25-cm-diameter sphere is about 0.64 N. The actual buoyancy force on a BL object can range anywhere from that value down through zero to negative values (positive net force downwards), depending on the temperature, particle mass density and number density, and other factors. Theories seem improbable which assume a high internal gas or plasma temperature leading to a mass density much less than air, and then propose that the mass of particulates inside the object is "just right" to counterbalance the buoyancy of the hot plasma or gas, because the chances are small that a random assembly of plasma and particles will always produce an average density approximating that of air. The more likely case seems to be that the air or gas inside the BL object is close to ambient pressure and temperature, and is decoupled by some means from the high electron or ion temperatures required to produce the observed plasma line or continuum radiation, and/or the high-temperature incandescent particles or aggregates which may also contribute to visible light emission.

The problem remains of determining how a plasma originating primarily from air (whether dusty or not) is subject to a power density ranging from 1.2 to 60 kW m^{-3} or more for the duration of the BL object's light emission. (These figures result from dividing the estimated power input of 10 to 500 W by the volume of a 25-cm-diameter sphere.) While this problem is not the focus of this paper, a brief review of some leading candidate mechanisms should mention the following:

(1) *Combustion*. In their paper proposing the oxidizing-silicon-nanoparticle theory to explain BL, Abrahamson and Dinniss (2000)) estimate that the combustion mechanism they describe could provide a power density as high as 79 kW m^{-3}, which exceeds the estimates in this paper for the power density required to account for light emission by incandescent particles. The main drawback to this theory is that no one has yet experimentally verified the proposed mechanism, although burning mm-size spheres of silicon or other metallic elements may account for a small percentage of ball-lightning observations (Stephan and Massey, 2008).
(2) *High-temperature plasma*. A number of researchers have published theories which attempt to explain BL with the creation of a high-temperature plasma by various means. One example is the theory proposed by Shmatov (2003) in which high-velocity electrons (up to 200 keV) oscillate around a core of low-velocity ions. Fusion plasma researchers are familiar with the fact that in high-energy plasmas, dust particles (often carbon ablated from chamber walls) can easily reach temperatures of 2000 K or more, emitting incandescent light in the process (Pigarov et al., 2005). While the energy source for the maintenance of such a plasma in naturally occurring BL objects remains elusive, the mechanism of energy transfer from the plasma to the particles is well known and experimentally verified. Attempts have been made to account for the source of a high-intensity electromagnetic field which might produce the plasma in question through the mechanism of maser action involving water or hydroxyl molecules (Handel and Leitner, 1994), but so far these theories also lack repeatable experimental verification. If the particle density were low enough, convective losses of heat from the particles to the surrounding air might be small enough to avoid significant visible convection of the object as a whole, especially if the plasma or its associated fields were subject to stronger forces than convection.

A "reality check" on the power-density calculations above can be obtained from some experiments performed independently by Dikhtyar and Jerby (2006) and this author (Stephan, 2006), involving the production of an atmospheric-pressure plasma in air with high-power 2.45-GHz microwaves. Approximating the resulting plasmoid by a 2-cm-diameter sphere, and recognizing that the minimum total applied power required to produce the plasmoid was on the order of 400 W, the average volumetric power density in the microwave fireball was about 12 MW m^{-3}, about two orders of magnitude greater than what we have estimated is required for naturally occurring BL objects. We would therefore expect the microwave plasmoid to be roughly two orders of magnitude brighter than the reported luminous intensity of BL objects. This is consistent with qualitative observations of the microwave plasmoid, which was so bright that welding goggles were usually needed to view it for any length of time. Spectral analysis of the emission from the plasmoid revealed that, except for a single line in the UV attributable to the hydroxyl radical, the spectrum was a fairly flat continuum, implying that either bremsstrahlung radiation from free electrons, or hot particles and clusters may have been the dominant emission mechanisms in these microwave-powered objects. Further investigation would be required to confirm this, however.

8. Conclusions

Beginning with a few visual characteristics common to many BL objects described in eyewitness reports, we have shown that the visual appearance of BL has quantitative implications for the means by which it produces light. We have examined two distinct mechanisms of light production: (1) the excitation (by unstated means) of a plasma to produce line and continuum radiation, and (2) the heating of small ($\sim$75-nm) particles or fractal aggregates of light-absorptive material (carbon in the examples shown), which in turn incandesce to produce the observed light emission.

We have shown that both of these mechanisms, either independently or in combination, can account for the observed range of intensities of BL objects in the great majority of cases. If allowance is made for both plasma emission (which tends to be primarily blue in atmospheric-pressure air due to excitation of molecular nitrogen) and the variation of emissivity with wavelength for different chemical compositions and particle structures, it is possible to account for the relatively wide variation in reported BL colors: red-orange, yellow, white, blue, purple, and almost any other reported color except green. Interestingly, in a compilation of reported colors of BL taken from reports of 1497 eyewitnesses, green was reported only once (Smirnov, 1987), although in a later summary of additional reports, green was reported 30 out of 1830 times (Amirov and Bychkov., 1994). Since green is the color emitted by the excited atoms of several metals (e g., copper), it is possible that the small number of green BL objects reported may be accounted for if evaporation from metal objects is considered. It is likely, though, that most BL light emission can probably be accounted for by a combination of plasma and chemical-reaction emissions and the incandescence of embedded particles or aggregates of particles.

While these results do not provide a full explanation for how BL objects emit light, they do trace the probable causal chain back from raw observational data to either plasma excitation or particle heating or both. Furthermore, they do so in a way which has been verified quantitatively with both eyewitness accounts of BL objects and with assumed values for the absorptivity and size of particles that are consistent with experimental results in other fields. It is hoped that these results will guide the future efforts of both experimenters trying to reproduce ball lightning in the laboratory, and theorists trying to account for one of the most mysterious of the remaining unsolved problems in atmospheric physics.

References

Abrahamson, J., Bychkov, A.V., Bychkov, V.L., 2002a. Recently reported sightings of ball lightning: observations collected by correspondence and Russian and Ukranian sightings. Philosophical Transactions of the Royal Society of London, Series A 360, 11–35.

Abrahamson, J., 2002b. Ball lightning from atmospheric discharges via metal nanosphere oxidation: from soils wood or metals. Philosophical Transactions of the Royal Society of London, Series B 360, 61–88.

Abrahamson, J., Dinniss, J., 2000. Ball lightning caused by oxidation of nanoparticle networks from normal lightning strikes on soil. Nature 403, 519–521.

Amirov, A.K., Bychkov, V.L., 1994. ANOVA of several parameters of the SKB data bank on ball lightning. Physica Scripta 50, 93–96.

Barry, J.D., 1980. Ball Lightning and Bead Lightning. Plenum, New York.

Bychkov, V., 2010. Artificial and natural fireballs as combustion objects. IEEE Transactions on Plasma Science 38, 3289–3290.

Charman, W.N., 1979. Ball lightning. Physics Reports 54, 261–306.

Dikhtyar, V., Jerby, E., 2006. Fireball ejection from a molten hot spot to air by localized microwaves. Physical Review Letters 96, 045002.

Egorov, A.I., Stepanov, S.I., 2002. Long-lived plasmoids produced in humid air as analogues of ball lightning. Technical Physics 47, 1584–1586.

Grigor'ev, A.I., Grigor'eva, I.D., Shiryaeva, S.O., 1992. Ball lightning penetration into closed rooms: 43 eyewitness accounts. Journal of Scientific Exploration 6, 261–279.

Handel, P.H., Leitner, J.-F., 1994. Development of the maser-caviton ball lightning theory. Journal of Geophysical Research 99, 10,689–10,691.

Ishimaru, A. 1978. Wave Propagation and Scattering in Random Media. IEEE Press, Piscataway, NJ (reissued ed. 1997).

Jennison, R.C., 1969. Ball Lightning (letter). Nature 224, 895.

Liu, L., Mishchenko, M.I., Arnott, W.P., 2008. A study of radiative properties of fractal soot aggregates using the superposition T-matrix method. Journal of Quantitative Spectroscopy and Radiative Transfer 109, 2656–2663.

Markel, V.A., Pustovit, V.N., Karpov, S.V., Gerasimov, V.S., Isaev, I.L., 2004. Electromagnetic density of states and absorption of radiation by aggregates of nanospheres with multipole interactions. Physical Review B 70, 054202.

Pigarov, A.Y., Krasheninnikov, S.I., Soboleva, T.K., Rognlien, T.D., 2005. Dust-particle transport in tokamak edge plasmas. Physics, Plasmas 12, 122508.

Purcell, E.M., 1969. On the absorption and emission of light by interstellar grains. Astrophysics Journal 158, 433–440.

Rakov, V., Uman, M.A., 2003. Lightning: Physics and Effects. Cambridge Univ. Press, Cambridge, UK.

Schuster, A., 1905. Radiation through a foggy atmosphere. Astrophysics Journal 21, 1–22.

Schnaiter, M., Gimmler, M., Llamas, I., Linke, C., Jäger, C., Mutschke, H., 2006. Strong spectral dependence of light absorption by organic carbon particles formed by propane combustion. Atmospheric Chemistry and Physics Discussions 6, 1841–1866.

Shmatov, M.L., 2003. New model and estimation of the danger of ball lightning. Journal of Plasma Physics 69, 507–527.

Shukla, P.K., 2001. A survey of dusty plasma physics. Physics of Plasmas 8, 1791–1803.

Singer, S., 1971. The Nature of Ball Lightning. Plenum, New York.

Smirnov, B.M., 1987. The properties and the nature of ball lightning. Physics Reports 152, 177–226.

Smirnov, B.M., 1993. Radiative processes involving fractal structures. Physics-Uspekhi 36, 592–603.

Sorensen, C.M., 2001. Light scattering by fractal aggregates: a review. Aerosol Science and Technology 35, 648–687.

Stenhoff, M., 1999. Ball Lightning: An Unsolved Problem in Atmospheric Physics. Kluwer, New York.

Stephan, K.D., 2006. Microwave generation of stable atmospheric-pressure fireballs in air. Physical Review E 74, 055401(R).

Stephan, K.D., Massey, N., 2008. Burning molten metallic spheres: one class of ball lightning? Journal of Atmospheric and Solar-Terrestrial Physics 70, 1589–1596.

Van Nes, F.L., Bouman, M.A., 1967. Spatial modulation transfer in the human eye. Journal of the Optical Society of America A: Optics, Image Science, and Vision 57, 401–406.

Versteegh, A., Behringer, K., Fantz, U., Fussman, G., Jüttner, B., Noack, S., 2008. Long-lived plasmoids from an atmospheric water discharge. Plasma Sources Science and Technology 17, 024014.

Wyszecki, G., Stiles, W.S., 1982. Color Science: Concepts and Methods, Quantitative Data and Formulae. Wiley, New York.